JEB
Journal of Environmental Biology

Journal Home page : www.jeb.co.in
E-mail : editor@jeb.co.in

ISSN: 0254-8704 (Print)
ISSN: 2394-0379 (Online)
CODEN: JEBIDP

Determination of seasonal changes in wetlands using CHRIS/Proba Hyperspectral satellite images: A case study from Acıgöl (Denizli), Turkey

Muhittin Karaman[1], Murat Budakoglu[1], Z. Damla Uca Avci[2], Emre Ozelkan[3], Ali Bulbul[4], Melda Civas[4] and Suat Tasdelen[4]*

[1]Geochemistry Research Group and JAL Laboratories, Department of Geological Engineering, Faculty of Mines, Istanbul Technical University, Istanbul-34460, Turkey

[2]Department of Astronautical Engineering, ITU Faculty of Aeronautics and Astronautics Engineering, Istanbul Technical University, Istanbul-34460, Turkey

[3]Agricultural and Environmental Informatics Research Center, Istanbul Technical University, 34460, Turkey

[4]Department of Geological Engineering, Pamukkale University, Denizli, 20070, Turkey

*Corresponding Authors Email : stasdelen@pau.edu.tr

Publication Info

Paper received:
10 July 2013

Revised received:
20 October 2013

Re-revised received:
18 June 2014

Accepted:
22 September 2014

Abstract

The changes in wetlands that occur through natural processes, as well as through industrialization and agricultural activities, are decreasing and even annihilating the living spaces of endemic species. Acıgöl (Denizli, Turkey), which is a suitable habitat for flamingos (*Phoenicopterus ruber*), is a lake that is affected by seasonal anomalies as a result of being shallow. Acıgöl, which is fed by precipitation, groundwater and the springs that occur along tectonic faults, has no water output other than evaporation and industrial activities. In addition to natural factors, it is important to determine the changes in the wetlands of Acıgöl, where industrial salt is produced, in order to reveal the micro-ecological equilibrium, the relationship between climate and natural life, and regulation of industrial activities. Remote sensing tools are frequently used in determination of changes in wetlands. Changes in coastlines, water level and area covered by water are parameters that can be examined by remote sensing while investigating wetlands. In this study, the water-covered area was examined using remote sensing. Within the scope of this study, CHRIS/Proba Mode 2 (water bandset) hyperspectral satellite images, acquired on 9/17/2011 for the season and on 6/18/2012 - 6/19/2012 for wet season, were used in order to present the seasonal changes in Acıgöl, during one hydrogeological period. The processes of noise reduction, cloud screening, atmospheric correction, geometric correction, and identification of wetlands have been implemented on the CHRIS/Proba images. In determining the water-covered areas, the Normalized Difference Water Index (NDWI) was used. It was determined that W6 (560 nm) and W18 (1015 nm) and W2 (447 nm) and W18 (1015 nm) band combinations were most appropriate to be used in NDWI to demonstrate the water-land separation. Using Proba-NDWI image, it was established that an area of 27.4 km^2 was covered with water during dry season, and 61.2 km^2 was covered during wet season. The results indicated that; since the lake water area is directly affected by seasonal and annual climatic anomalies, water used by industrial facilities has to be drawn out of the lake in reasonable amount.

Key words

Wetland, CHRIS/Proba, Wet and dry season, Water-covered area change, Proba-NDWI

Introduction

The changes occurring in wetlands, which hosts many endemic species, are of great importance environmentally and ecologically (Ozturk and Secmen, 1986; Ozturk *et al.*, 1996). Continuous efforts to track and conserve these ecosystems should be placed in particular importance for regions where human factors such as industrialization and agricultural activities

have an impact on the area, in addition to factors of natural origins (Gucel *et al.*, 2012; Altay and Ozturk, 2012).

Acıgöl Lake provides suitable living space for flamingos and has significant value, as it is placed in Class B conservation category (Karadeniz Tiril, and Baylan, 2009). The chemical characteristics of lake water provides living space for various micro and macro organisms that have adapted to this environment (Kilic and Eken, 2004; Balkiz *et al.*, 2009). Besides its ecological characteristics (Karaman *et al.*, 2011a), the lake is one of Turkey's most important industrial wetlands due to its contribution in salt and sodium sulfate production (Gundogan *et al.*, 1995). As a part of this production process, water is drawn out of the lake. However, uncontrolled drawing can damage the natural equilibrium of the lake. The amount of water drawn out should be carefully calculated, considering that the water may change due to seasonal climatic conditions; and in total, water had to be kept within reasonable levels (Karaman *et al.*, 2011b).

The changes occurring in water level of a lake can be monitored by satellite remote sensing techniques. The coastline, water level, and water-covered area are frequently used parameters in the change detection analysis of lakes (Ekercin, 2007; Reis and Yilmaz, 2008; Sener *et al.*, 2009; Karsli *et al.*, 2011; Yildirim *et al.*, 2011). For extraction of water, the methods used are density slicing, thresholding (Frazier and Page, 2000; Jain *et al.*, 2005), and indices such as Normalized Difference Water Index (NDWI) (Gao, 1996; McFeeters, 1996; Jain *et al.*, 2005; Xu, 2006; Karsli *et al.*, 2011; Zhao *et al.*, 2011; Sun *et al.*, 2012; Lyons *et al.*, 2013; Li *et al.*, 2013) and Normalized Difference Pond Index (Lacaux *et al.*, 2007). In the thresholding method, specific thresholds are defined for each study case. Uncertainty in values originate from intrinsic water characteristics of lakes under investigation, and the land cover complexity of surrounding environments (Xu, 2006; Ji*et al.*, 2009; Campos *et al.*, 2012). Despite a considerable number of studies, there have been divergent opinions about the selection of index and establishment of thresholds (Ouma and Tateishi, 2006; Lacaux *et al.*, 2007; Zhang*et al.*, 2008; Soti*et al.*, 2009).

NDWI uses a combination of two-band math. This operation enhances the water spectral signals by contrasting the reflectance between different wavelengths, and removes a large portion of noise components in order to effectively reveal water delineation (Ji *et al.*, 2009; Campos *et al.*, 2012). The near-infrared (NIR) band has been referenced as well suited for detection of open water areas from satellite images, since water has a stronger absorptive capacity in the NIR range than land does (Mc Feeters, 1996; Verdin, 1996). The middle-infrared (MIR) band is also efficient for open water area detection, since water has a high MIR absorption, and other landscape components have a higher reflectance of MIR than NIR (Gao, 1996; Xu, 2006). Several NDWIs composed of NIR and MIR combinations have been proposed. The most frequently used NDWIs are (Campos *et al.*, 2012): (1) $NDWI_{NIR/MIR}$ = (NIR - MIR) / (NIR + MIR) (Gao, 1996); (2) $NDWI_{G/NIR}$ = (green - NIR) / (green + NIR) (McFeeters, 1996); and (3)the modified NDWI, $NDWI_{G/MIR}$ = (green - MIR) / (green + MIR) (Xu, 2006). In this study, all possible NDWI combinations were tested, and the most appropriate two-band combinations, here named as Proba-NDWI, were selected for determination of water-covered area.

In the present study, the seasonal change in water-covered area of Acıgöl lake was examined by using hyperspectral multi-angular CHRIS/Proba satellite images acquired in Mode 2. CHRIS/Proba provides relatively new data among the present sensors, and its performance is being investigated in many studies. It has various imaging modes, one of which is designed for acquiring data in the wavelength interval known as water bands (Mode 2). CHRIS/Proba data, due to its high spatial and spectral resolution, is advantageous for water studies when compared with ocean color satellite sensors and hyperspectral airborne sensors (Giardino *et al.*,2013).

In order to demonstrate the seasonal changes within a year, a September 2011 image presenting dry season, and two June 2012 images presenting wet season were used. The water-covered areas on different seasons were obtained by NDWI.

After attaining the difference in water-covered area, the Thornthwaite method, which can be used to demonstrate water balance for long-term period (Keim, 2010), was applied using meteorological data gathered from the Cardak (Denizli, Turkey) Weather Station. Given monthly mean temperature from meteorological station, estimation of potential evaporation for each month of the year can be output by using Thornthwaite method.

The rate of change in water-covered area was obtained by using satellite images, and then combining it with potential evapotranspiration value estimated by Thornthwaite method. All the data were analyzed to understand the dominant parameters of change in lake water.

Materials and Methods

Study area : The study area is located in Denizli and Afyon provinces, between 37°55'27.98" N - 37°45'7.41" N latitude and 30° 0'17.24" E - 29°41'11.72" E longitude (Fig. 1).

Lake Acıgöl, which consists of karstic springs (Mutlu *et al.*,1999), is at the center of 1,609 km^2-wide Acıgöl Basin, and at an altitude of 836 m (Akar *et al.*, 2012). During the wet season, groundwater (Mutlu *et al.*,1999), superficial currents and the Kocacay stream feed the lake. In addition to these sources, there is an input of water into the lake coming from many large and small seasonal or permanent springs situated along the Acıgöl fault line on the south (Mutlu *et al.*,1999). The most important springs are the Akpinar and Gemis ones(Karaman *et al.*, 2011b).

Acıgöl is a closed lake and the water output is evaporation,however, water is drawn from the lake for industrial purposes (Mutlu *et al*.,1999; Karaman *et al.*, 2011a).

Acıgöl is a natural lake that supplies the production of 85% of Turkey's sodium sulfate demand (Gundogan *et al.*, 1995; Mutlu *et al*.,1999). Sodium sulfate and salt are produced from the lake by natural and refining methods. Shallow artificial salt evaporation ponds have been created inside the lake for this purpose (Karaman*et al.*, 2011c). The lake has been used since 1953 for this production; mining activities have been continuing to grow and spread to larger areas (Karaman *et al.*, 2011d).

The long-term annual total precipitation at Lake Acıgöl is 384.64 mm, and the average air temperature is 13.39^{0}C. The maximum average long-term air temperature at the lake is 24.56 ^{0}C in July, and for long term, the highest precipitation value is observed as 47.17 mm in December.

Satellite data : CHRIS/Proba is a satellite that has been developed by ESA (European Space Agency) and the British National Space Center funds to be used for environmental studies, and recently sent into space. It carries a hyperspectral sensor, and efforts are currently being made by numerous researchers to use it for various applications. The satellite acquires data in 5 different modes. Modes 1, 2, 3, 4, and 5 have 62, 18, 18, 18, and 37 bands, respectively. The bandwidth of the modes are 406-992, 406-1003, 438-1035, 486-788 and 438-1003 nm, and they are generally used for agriculture, water, earth, chlorophyll, and earth studies (Cutter, 2008). For this study, Mode 2 images were obtained. Mode 2 consists of a bandset which is mainly designed to be used in water studies. The water bandset properties are given in Table 1.

Within the scope of this study, CHRIS/Proba images acquired on September 17th, 2011; June 18th, 2012; and June 19th, 2012 were used. While the image dated 9/17/2011 covers the lake area, in June 2012, the lake area could only be imaged on consecutive days in two frameworks. Since CHRIS/Proba has a multi-angular acquisition capability, 9/17/2011 image was acquired with acquisition angles 55, 36, 0, -55, and -36, a 6/18/2012 image was acquired with acquisition angles of 55, 36, 0 and -36, and a 6/19/2012 image was acquired with acquisition angles of 55, 36, 0, -55 (Fig. 2), respectively. The images were in HDF4 format and calibrated.

The Chris Toolbox for BEAM-Tool, which was developed on behalf of ESA, was used to process CHRIS/Proba images. Firstly, noise reduction procedures were applied to the images. Following this, cloud screening and atmospheric correction were implemented. After geometric correction, NDWI indices were generated in order to identify the water areas. The image processing steps of determining the lake area are presented in Table 2. After obtaining the final images, the lake water area, and its change in time were interpreted by Thornthwaite method.

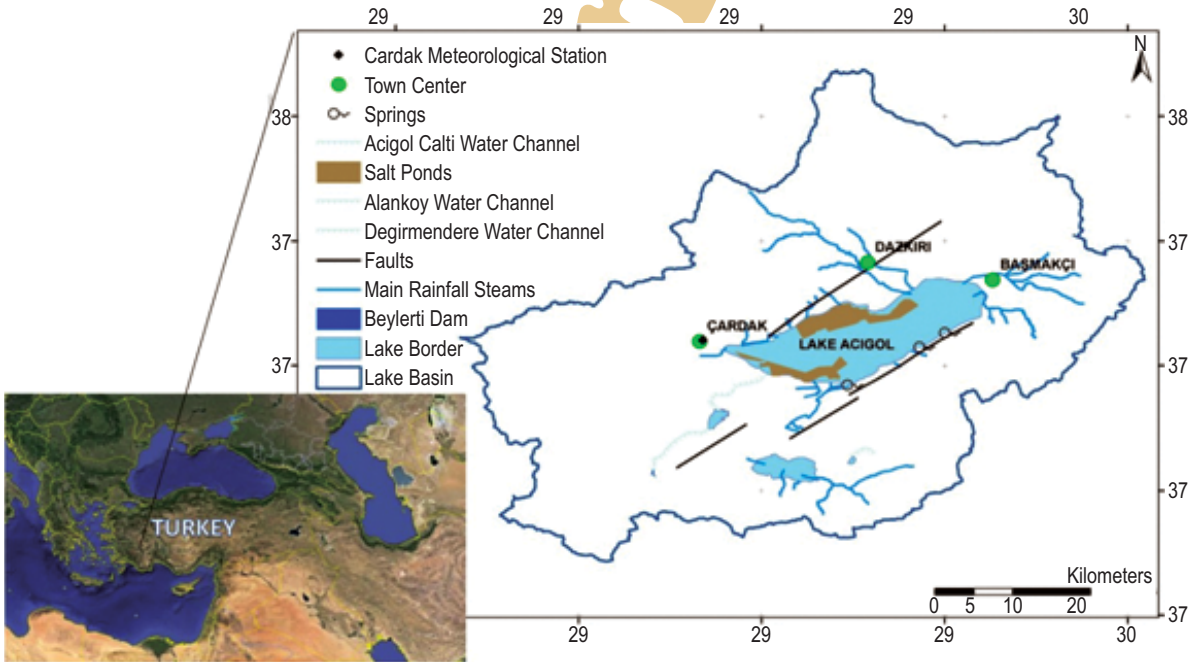

Fig. 1 : Study area

Table 1 : CHRIS/Proba band properties for Mode 2 (nm) (Cutter, 2005; 2008)

Band	Min	Average	Max	Width
W1	406	411	415	10
W2	438	442	447	9
W3	486	490	495	9
W4	505	510	515	10
W5	526	530	534	9
W6	556	561	566	10
W7	566	570	577	8
W8	585	590	596	12
W9	618	622	627	9
W10	646	651	656	10
W11	666	672	677	11
W12	677	680	683	6
W13	683	686	689	6
W14	700	706	712	12
W15	752	755	759	7
W16	773	781	788	15
W17	863	872	881	18
W18	1003	1019	1036	33

Image processing

Noise reduction : Noise reduction in images was achieved by using the algorithm developed by Gómez-Chova*et al.* (2008). In the images, noise signals of drop-out and vertical striping were detected and corrected.

Cloud screening : The cloud screening algorithm was conducted in several phases, which are TOA (top-of-atmosphere) reflectance, feature extraction, image clustering, cluster labeling, and spectral unmixing. At TOA reflectance step, the illumination conditions were calculated with a new reflectance value using the acquisition date and angle as inputs (Brockman, 2013). In the application, cloud screening was performed by 14 clusters, by 30 iterations using the whiteness and brightness values of NIR band.

Atmospheric correction : For atmospheric correction, the atmospheric correction tool, developed by Guanter *et al.*(2005a; 2005b) (Brockman, 2013),was used which as follows: spectral calibration (CHRIS/Proba modes 1-5); retrieval of the aerosol optical thickness (AOT); retrieval of data on columnar water vapor (CHRIS/Proba Modes 1, 3, and 5) (CWV); retrieval of surface reflectance and spectral polishing (removal of systematic errors in surface reflectance) (CHRIS/Proba Modes 1-5).

The atmospheric correction module uses MODerate resolution TRANsmittance (MODTRAN4) algorithm developed by Berk *et al.* (2003). The AOT at 550 nm, which is accepted as a basic wavelength for correction, was computed as 0.143 for the image on 9/17/2011. As Mode 2 image does not provide reflectance data on 940 nm, which is at the center of water absorption region, the columnar water vapor density was taken as 1.0 $g*cm^{-2}$. The cloud product threshold was assumed to be 0.05. When CHRIS/Proba Mode 2 image was taken, in addition to the spectral characterization update and the spectral polishing and data retrieval on the columnar water vapor operations, the atmospheric correction was also realized by retrieval of AOT and surface reflectance.

After the above data was realized, the difference in spectral reflectance, that occurred before and after the atmospheric correction on different natural field objects, were assessed for sampling points located as shown in Fig. 3 and defined in Table 3. The spectral curves of chosen sample points, representing different land cover classes were obtained from the processed image; indicated on Fig. 4 and 5, respectively, for before and after the atmospheric correction situations.

Geometric correction : Thegeometric correction was conducted by using first degree polynomial transformation method on transformation into WGS 84 datum, UTM projection system, and the nearest-neighbor method was chosen for resampling. Table 4 shows the number of ground control points (GCP) used, and the root mean square error (RMSE) values calculated for each image.

Identification of water area

Producing Image Mosaic : The image mosaicking was performed on the June 2012 dated images. Two complementing images having the same viewing angles were used. The mosaic images generated from the available June 2012 images (0 and 36 degrees) are demonstrated in RGB: 9, 8, 7 color combination in Table 5.

Table 2 : Theimage-processing steps followed in determining the lake area

Noise reduction	Cloud screening	Atmospheric correction	Geometric correction	Identification of water area
* Drop-Out correction	* TOA Reflection	* Update of spectral characterization	* Localizing Ground Control Points	* Producing Image Mosaics
* Vertical striping	* Feature Extraction	* Aerosol optical thickness (AOT) retrieval	* Projection Specification	* Production of Proba-NDWI images
	* Image Clustering	* Columnar water vapor (CWV) retrieval		
	* Cluster Labeling	* Surface reflectance retrieval		
	* Spectral Unmixing	* Spectral polishing		

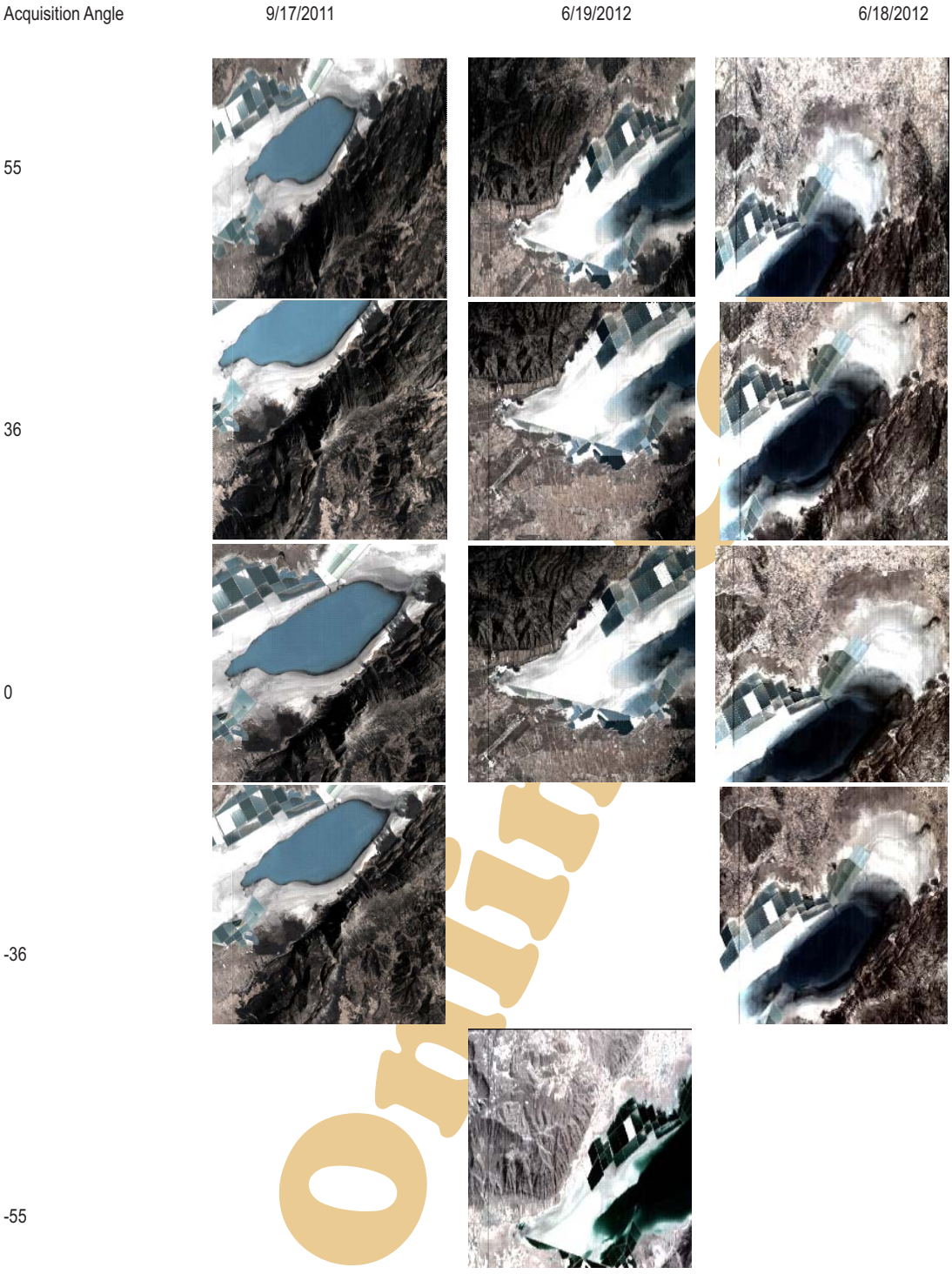

Fig. 2 : CHRIS/Proba images used

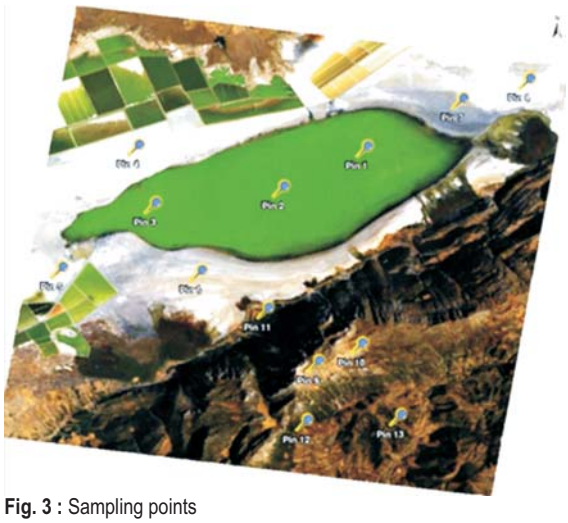

Fig. 3 : Sampling points

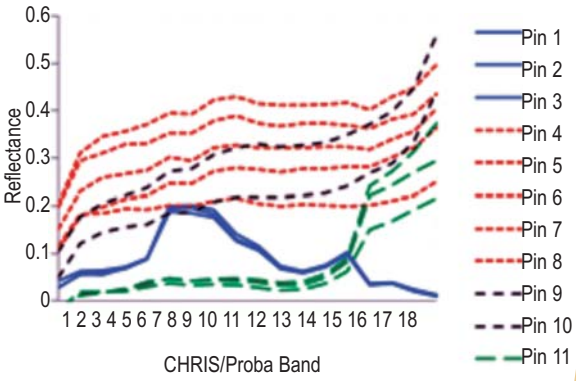

Fig. 5 : Reflectance curves after atmospheric correction

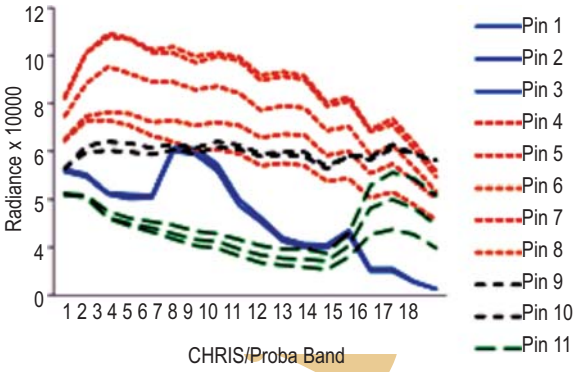

Fig. 4 : Radiance curves before atmospheric correction

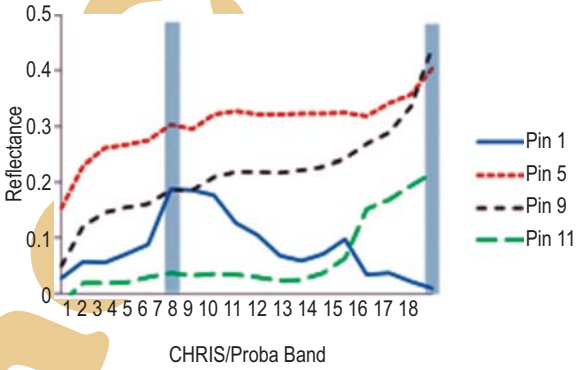

Fig. 6 : Spectral library of different land covers from CHRIS/Proba satellite images

Identification of the lake area with Proba-NDWI : After the mosaic images were formed, NDWI, which was developed by McFeeters (1996) and Gao (1996) for identification of water components, was applied. At first, the widely used NDWI indices, which are demonstrated in Table 6, were examined.

The proper NDWI wavelengths were determined by applying the two steps given below: Spectral library, which consists of lake water, lake sediment, rock, and vegetation classes, was created from atmospherically corrected CHRIS/Proba images using the spectral reflectances at sample points (Fig. 6). While lake water showed the highest reflectance on 6th band (560 nm) and lowest reflectance on 18th band, lake sediment, rock, and vegetation had highest reflectance on 18th band (1015 nm); The NDWI values for each possible band combination were calculated. It was observed that water sample had positive values, and other land forms had negative values when W2 and W18, W2 and W15, W6 and W18, W6 and W15, W15 and W18 band combinations were used. In Table 7, the derived NDWI values for most appropriate band combinations mentioned above were given for each test point. At bottom line of the table, variance values of NDWI for each of the land cover classes, which exhibit variety in a dataset, were given. The values indicate that the best band combination among them were W6 and W18 and W2 and W18.

After examining Table 7, the Proba-NDWI index was created with an adaptation of the reflectance values of band W18 (1015 nm) and band W6 (560 nm):

$$\text{Proba-NDWI} = (W6-W18) / (W6+W18)$$

According to NDWI value table (8), masking was applied to NDWI images, in order to separate the water-covered areas from the other land cover classes. The resultant images were classified as water-covered areas (1), non-water-covered areas (0), and each class was transformed into different vectors. Between the dry and wet seasons, a growth of 123.32% was observed in the lake area (Fig. 7).

Table 3 : Sampling points of different spectra

Points	Land cover	Points	Land cover
Pin1	Lake Water	Pin7	Lake Sediment 2
Pin2	Lake Water	Pin8	Lake Sediment 2
Pin3	Lake Water	Pin9	Rock
Pin4	Lake Sediment 1	Pin10	Rock
Pin5	Lake Sediment 1	Pin11	Vegetation
Pin6	Lake Sediment 1	Pin12	Vegetation
		Pin13	Vegetation

Table 4 : Number of GCPs and RMSE in the geometric correction

Screening date	Viewing angle (º)	# GCP	RMSE
17.09.2011	0	16	0.5
	-36	8	0.7
	+55	7	1
	-55	7	1
18.06.2012	0	7	0.6
	36	6	1.0
	-36	5	0.4
	55	6	0.9
19.06.2012	0	6	0.8
	36	7	0.7
	-36	5	0.8
	55	6	0.9

The lake area on June 2012 could be identified only from the images with viewing angles of 0 and +36 degrees, while it could be identified from all viewing angles except +36 for September 2011. To compare the results and have an idea of CHRIS/Proba's performance, the water-covered areas were calculated for each angle image. At acquisition angles other than +55 degrees, very close values were obtained.

The Thornthwaite method and hydrological water budget : Thornthwaite method employs the hydrological water budget chart in computation of evapotranspiration, and the climate type is also identified with this chart (Thornthwaite, 1948). This classification method is frequently used in various applications that relate to evapotranspiration, such as agriculture, hydrogeology and water resources management (Thornthwaite, 1948; Bailey *et al*.,2014; Gulsoy *et al*, 2014; Varol and Davraz, 2014).

The steps of Thornthwaite method are as follows:

$$i = \left(\frac{t}{5}\right)^{1.514} \rightarrow I = \sum_{n=1}^{n=12} i \rightarrow ET_p = 16\left(\frac{10t}{I}\right)^{a} xG$$

where, ET_p = Potential monthly evapotranspiration (mm/month); t = Monthly average temperature (°C); I = Annual temperature index equal to summation of indices (i) of 12 months; a = (is a coefficient) = $(675 \times 10^{-9}) I^3 - (771 \times 10^{-7}) I^2 + (179.21 \times 10^{-4}) I + 0.49293$; G = Circle of latitude correction coefficient.

Table 5 : Themosaic images generated from 6/(18 & 19)/2012 (RGB: 9, 8, 7).

Viewing Angle (º)	Pixel Image
0	
36	

The required meteorological data were taken from the Cardak Weather Station of the Turkish State Meteorological Service (TSMS). It was thought that the meteorological data measured at this station can represent Acıgöl by being close to the region with regards to location and elevation. The average temperature and aggregate precipitation data were used. The values of potential evapotranspiration (ET_P) and actual evapotranspiration (ET_R) were computed from the data between the years 1964–1991 (27 years), and the years 2007–2008, as a base. According to this method, the yearly ET_P at Cardak was derived as 831.37 mm, while the ET_R was found to be 372.01 mm. The monthly change in average precipitation, temperature, ET_R, and aggregate ET_P are given in Fig. 8.

During study period, from middle October till last week of April at Acıgöl, precipitation was higher than ET_P, therefore, ET_P equal to ET_R. From the beginning of June till mid October there was shortage of water at Acıgöl. During this period of dry season at Acıgöl where ET_P was higher than precipitation, ET_P was 734.6 mm, while precipitation was 175.24 mm. With high role of precipitation, the entire ground water reserve of 100 mm was evaporated. Thus, deficit of water was computed as 734.36-(175.24+100) = 459.36 mm. The 100 mm ground water reserve began to fill up around mid October, and was completed at the beginning of February of the following year. At Cardak, the average annual precipitation of 384.64 mm and

Table 6 : TheNDWI water indices for Landsat 5 - TM images [P: (nm) wavelength] (Karaman *et al.,* 2011d, Campos *et al.,* 2012)

Name of Indices	Name of Method	Algorithm Formula
NDWI	Gao, 1996	(P860-P1240) / (P860+P1240)
NDWI	McFeeters,1996	(P560-P830) / (P560+P830)
NDWI	Xiao *et al.,* 2002	(P(780-890) - P(1580-1750)) / ((P(780-890) + P(1580-1750))
NDWI	NSIDC, 2002Thomas and Michael, 2003	(P(750-900) - P(1550-1750)) / (P(750-900) + P(1550-1750))
NDWI	Kaneko *et al.,* 2002	(P(630-690) - P(1550-1750)) / (P(630-690) + P(1550-1750))
NDWI	Rogers and Kearney, 2004	(P(630-690) - P(1550-1750)) / (P(630-690) + P(1550-1750))
MNDWI	Xu, 2006	(P560- P1650) / (P560+P1650)

Table 7 : Theaverage NDWI values of the corresponding Pin Classes for different band combinations and the related variance value

Land Cover	W2 & W18	W2 & W15	W6 & W18	W6 & W15	W15 & W18
Lake water	+0.71	+0.25	+0.90	+0.70	+0.56
Lake sediment	-0.27	-0.16	-0.14	-0.03	-0.12
Rock	-0.57	-0.38	-0.41	-0.18	-0.24
Vegetation	-0.85	-0.79	-0.71	-0.61	-0.18
Variance	0.46	0.19	0.49	0.30	0.14

Table 8 : The pixel correspondences ofthe Proba-NDWI images

Proba-NDWI Value	Corresponding Land	Proba-NDWI
	Cover Class	Color Code
> 0	Water	White
≤ 0	Land	Grey-Black

Table 9 : The lake area (km) computed from different acquisition angles

Acquisition Angle (°)	Area (km^2)	
	September 2011	June 2012
-55	27.04	
-36	27.38	
0	27.40	61.19
36		61.50
55	25.94	

372.01 mm returned to atmosphere by evapotranspiration. The aggregate precipitation that occurred in January, February, and March (69.59 mm) was approximately 18% of the annual aggregate precipitation. Methodologically, the evapotranspiration values obtained here represent the amount of : vaporization from the precipitation before it reaches the ground; vaporization from the ground and vaporization from the shallow depths. This depth, which may be defined as reachable by plant roots, depends on the flora and lithology. Before soundly interpreting the evaporation in Acıgöl, evaporation pan observations geared towards computation of evaporation from the free water surface of the lake is required.

Results and Discussion

CHRIS/Proba is a new data that is being used and investigated by many researchers to understand its performance. It has various imaging modes, one of which is designed for acquiring data in the wavelength interval known as water bands (Mode 2). In this application, it is shown that determination of water covered area and efficient use of NDWI index can be achieved using the CHRIS/Proba.

NDWI has been mostly applied on multispectral satellite images, as can be seen in the literature. It has been applied to a hyperspectral satellite image in this study. Due to the low spectral resolution of general multispectal data, NDWI has been defined with a wide-ranged visible and infrared band interval (Gao,1996; Xu, 2006). By using the hyperspectral data, it was possible to detect more accurate band intervals to define NDWI for this study. In addition to its high spectral resolution, CHRIS/Proba showed better spatial resolution as compared to widely used satellite data in ocean studies, and it reveded that CHRIS/Proba is a good data source for inland water studies.

In the present study, W2 and W18; W2 and W15; W6 and W18; W6 and W15; W15 and W18 band combinations were performed successfully for delineation of water-covered area; however, it was determined that W6 (560 nm) and W18 (1015 nm); W2 (447 nm) and W18 (1015 nm) were the most appropriate CHRIS/Proba bands to be used in NDWI index. Use of this bands in NDWI seems to be reasonable and also effective, while variance values were examined.

The characteristics of lake on acquisition season and time, the properties of satellite data and even the image

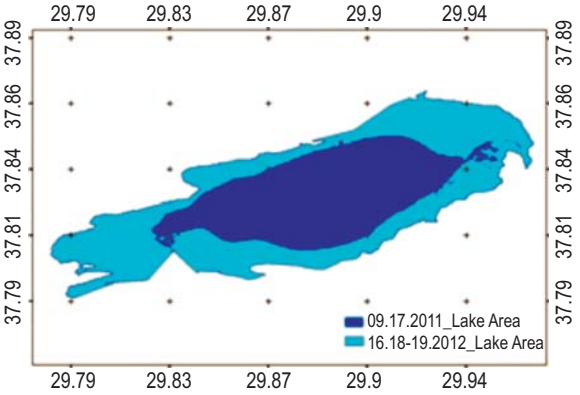

Fig. 7 : Water-covered area on September 2011 and June 2012

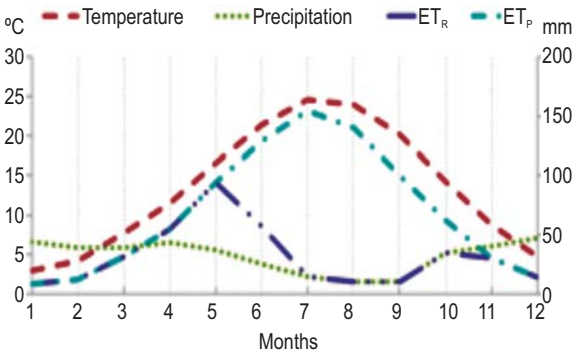

Fig. 8 : Derived meteorological data according to the TSMS statistical data (Karamanet al., 2011b)

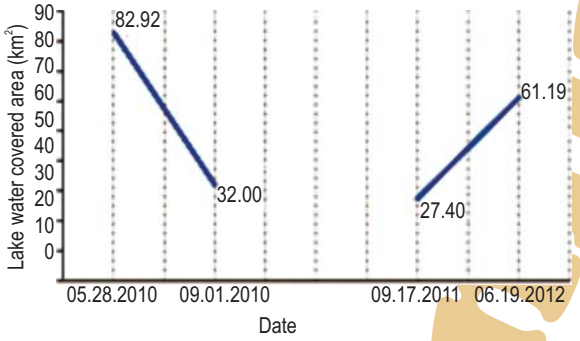

Fig. 9 : Changes of lake water covered areas in two hydrological periods between 2010 wet to 2012 wet from the Karaman *et al* (2011a) and the current study

preprocessing algorithms can effect detection of water-covered areas (Evan *et al.,* 2013). According to the findings of the current study, good identification of water surface in Visible-NIR region using Chris/PROBA was available in many band combinations due to its high spectral resolution. Additionally, better determination of water surface area may highly depend on lake's seasonal characteristics. Wenbo *et al.* (2013) examined optimum bands for water surface detection using multispectral Advanced Land Imager (ALI) data and reported similar results as Xu (2006): green (525-605 nm) and MIR (1550-1750). In the current study, optimum bands were found to be W6 (560 nm) and W18 (1015 nm), due to the capability of Chris/PROBA that did not have MIR sensor. As a result, the band combinations were obtained as W6 (560 nm) and W18 (1015 nm); W2 (447 nm) and W18 (1015 nm) for optimum NDWI indices.

The water-covered area calculations still resulted in approximate values for images acquired with 0 and ±36 acquisition angles. This finding demonstrates that in CHRIS/Proba studies, where a 0 degree image cannot be obtained, ±36 acquisition angled images can be used instead. Additionally,the multi-angular acquisition availability of the CHRIS/Proba can be an advantage for increasing the acquisition frequency of a region.

By reviewing previous studies, interpretations have been made about the lake water change in time. In a previous study conducted in 2011 using Landsat 5TM data, Karaman *et al.*, (2011a) demonstrated diminution in lake that occurred between 5/28/2010 and 9/1/2010, presenting wet and dry season. It was determined that the water-covered area at Acıgöl was diminished by 61.4% during the period of May-September 2010. On the contrary Karaman *et al.* (2011a) examined that from wet to dry season, in this study the changes from dry to wet season were examined. The current study showed that the lake area decreased from wet to dry season, and increased from dry to wet season which confirms the previous study of Karaman *et al.* (2011a) (Fig. 9).

Karaman *et al.* (2011b) reported that Acıgöl changes in the lake area were linearly related to evaporation R^2 = 0.9226, precipitation R^2 = 0.9198, and temperature R^2 = 0.6158 in the wetlands of Acigol. It was remarked that, besides meteorological effects, solution mining activities were also operative in the diminution of the lake area (Karaman *et al.*, 2011a, b).

The current and the previous studies showed that the major effects on lake water area changes are occurring due to industrial, meteorological and hydrological events. The meteorological events, such as decrease in precipitation or increase in vaporization during summer period, may have a significant impact on the changes and allocation of lake water, unless industrial affects are applied, considering the lake's fragile environment. Therefore, the authors concluded that these kinds of analyses have to be periodically done, and an accurate estimation of water limits to be drawn out of the lake has to be determined to inform the firms. Also, legislation to conserve the lake's environment should be passed that can make the firms comply to protect it.

The study emphasized that remote sensing is a useful technique for monitoring wetland systems to detect areal change of water-covered area. In the further studies; the temporal

changes in the lake area will be examined for longer periods and frequent seasons by considering more *in-situ* data that will define the lake characteristics. Additionally, hydrological events will be defined simultaneously with remote sensing analysis.

Acknowledgments

This study was supported by the 110Y255 TUBİTAK ÇAYDAG Project. The CHRIS/Proba images were procured with the support of ESA's project support, number C1P.6693. Authors thank the Ministry of Forestry and Water Affairs of the Republic of Turkey for granting research permit.

References

Akar, I., D. Maktav and N. Gunal: Determination of changes in lake surface using different digital image processing techniques (in Turkish). *Havacilikve Uzay Teknolojileri Dergisi*, **5**, 35-41 (2012).

Altay, A. and M. Ozturk: Halophytic plant diversity of Milleyha (Samandag-Hatay) freshwater ecosystem, land degradation due to human disturbances and conservation measures. *Paki. J. Bot.*, **44**, 37-50 (2012).

Balkız, O., U. Ozesmi, R. Pradel, C. Germain, M. Siki, J.A. Amat, M. Rendon Martos, N. Baccetti and A. Bechet: An update of the Greater Flamingo *Phoenicopterus roseus* status in Turkey. In: Flamingo, Bulletin of the IUCN-SSC/Wetlands International Flamingo Specialist Group, Special Publication 1 (Eds.: A. Béchet, M. Rendón-Martos, J. A. Amat, N. Baccetti, and B. Childress): Proceedings of the IV International Workshop on the Greater Flamingo in the Mediterranean region and northwest Africa. Wildfowl & Wetlands Trust, Slimbridge, UK. p. 30-33 (2009).

Bailey, R. T., A. Khalil, V. Chatikavanij: Estimating transient freshwater lens dynamics for atoll islands of the Maldives. *J Hydrol.*, **515**, 247-256 (2014).

Berk, A., G.P. Anderson, P.K. Acharya, M.L. Hoke, J.H. Chetwynd, L.S. Bernstein, E.P. Shettle, M.W. Matthew and S.M. Adler-Golden: MODTRAN4 Version 3 Revision 1, User's manual, Technical report. Air Force Research Laboratory, Hanscom Air Force Base, MA, USA (2003).

Brockman: http://www.brockmann-consult.de/beam/chris-box/beam-integration.html, Brockmann Consult, (23/4/2013).

Campos, J., N. Sillero and J.C. Brito: Normalized difference water indexes have dissimilar performances in detecting seasonal and permanent water in the Sahara–Sahel transition zone. *J. Hydro.*, 464–465, 438–446 (2012).

Cutter, M. A.: Chris Data Format Document. Issue 4.2, p. 2-31 (2005).

Cutter, M. A.: Chris Data Format rev1., p. 2-37 (2008).

Ekercin, S.: Coastline change assessment at the Aegean Sea coasts in Turkey using multitemporal Landsat imagery. *J. Coastal Res.,* **23**, 691–698 (2007).

Frazier, P. and K. Page: Water body detection and delineation with Landsat TM data. *Photogr. Eng. Remote Sens.,* **66**, 12 (2000).

Gao, B.: NDWI a normalized difference water index for remote sensing of vegetation liquid water from space. *Rem. Sen. Environ.,* **58**, 257–266 (1996).

Giardino, C., M. Bresciani,, D. Stroppiana, A. Oggioni and G. Morabito: Optical remote sensing of lakes: an overview on Lake Maggiore. *J. Limnology,* **73**, 201-214 (2013).

Gomez-Chova, L., L. Alonso, L. Guanter, G. Camps-Valls, J. Calpe and J. Moreno: Correction of systematic spatial noise in push-broom hyperspectral sensors: Application to CHRIS/Proba images. *Appl. Opt.,* **47**, 46-60(2008).

Guanter, L., L. Alonso and J. Moreno: A method for the surface reflectance retrieval from PROBA/CHRIS data over land: Application to ESA SPARC campaigns. IEEE Transactions on Geoscience and Remote Sensing, **43**, 2908-2917 (2005a).

Guanter, L., L. Alonso and J. Moreno: First results from the PROBA/CHRIS hyperspectral / multi angular satellite system over land and water targets. *IEEE Geosci. Rem. Sen. Lett.,* **2**, 250-254 (2005b).

Gucel, S., C. Kadis, O. Ozden, I. Charalambidou, C. Linstead, W. Fuller, C. Kounnamas and M. Ozturk: Assessment of biodiversity differences between natural and artificial wetlands in Cyprus. *Pak. J. Bot.,* **44**, 213-224 (2012).

Gundogan, I., C. Mordogan and C. Helvaci: Türkiye'deki acı göllerden sodyum sülfat üretimi (The production of sodium sulfate from brackish lakes in Turkey). Endüstriyel Hammaddeler Sempozyumu, Proceedings, p257-266, Izmir,Turkey (1995).

Jain, S.K., R.D. Singh, M.K. Jain and A.K. Lohani: Delineation of flood-prone areas using remote sensing techniques. *Wat. Res. Manag.,* **19**, 333–347 (2005).

Ji, L., L. Zhang and B. Wylie: Analysis of dynamic thresholds for the normalized difference water index. Photogram. *Eng. Remote Sens.,* **75**, 1307–1317 (2009)

Kaneko, M., M. Takada, K. Tsuchiya and H. Fukuma: The classification of vegetation of wetland based on remote sensing methods, over Kushiro wetland Hokkaido Japan. *Report of Hokkaido Institute of Environ. Sci.,* **29**, 53-58 (2002).

Karadeniz, N., A. Tiril and E. Baylan: Wetland management in Turkey: Problems, achievements and perspectives. *Afri. J. Agric. Rese.,* **4**, 1106-1119 (2009).

Karaman, M., Z. D. Uca Avci, I. Papila and E. Ozelkan: The analysis of destruction in flamingos habitat of Acıgöl Wetland. In: 34th International Symposium on Remote Sensing of Environment (ISRSE2011): The GEOSS Era: Towards Operational Environmental Monitoring , Sydney Convention & Exhibition Centre, Proceedings, p 1-4, N.S.W (2011a).

Karaman, M., Z. D. Uca Avci, M. Budakoglu, S. Tasdelen, E. Ozelkan and I. Papila: Flamingoların Beslenim Alanlarındaki Tahribatın Uzaktan Algılama Yöntemleri ile Değerlendirilmesi: Acıgöl (Denizli) Örneği (The analysis of destruction in a flamingo habitat by using remote sensing technology, A Case Study: Lake Acigol (Denizli)). II. Türkiye Sulak Alanlar Kongresi, Proceedins, 111-120, Kırşehir/Türkiye (2011b).

Karaman M., Z. D. Uca Avci, E. Ozelkan, M. Budakoglu: Çözelti Madenciliği Faaliyet Alanlarının Zamansal Değişiminin Uzaktan Algılama Yöntemleri ile Değerlendirilmesi: Acıgöl (Denizli) Örneği (Evaluation of temporal change in solution mining areas by using remote sensing, A case study : Acıgöl (Denizli)). 4.Madencilik ve Çevre Sempozyumu, 63-70, İzmir/Turkey, (2011c).

Karaman, M., M. Budakoglu, S. Tasdelen, Z. D. Uca Avci, A. Duman: Acıgöl'ün (Denizli) Uzaktan Algılama Yöntemleri ve CBS Kullanılarak Rezervinin Hesaplanması (Evaluation of Lake Acıgöl (Denizli) Reserve Using Remote Sensing and GIS Methods). II. Türkiye Sulak Alanlar Kongresi, Proceedings, 63-71, Kırşehir/Turkey (2011d).

Karsli, F., A. Guneroglu and M. Dihkan: Spatio-temporal shoreline changes along the southern Black Sea coastal zone. *J. Appl.*

Remote Sens., **5**, (2011).
Keim, B.: The lasting scientific impact of the Thornthwaite water-balance model. *Geographical Review,* **100**, 295–300 (2010).
Kilic, D. T. and G. Eken: Important bird areas of Turkey, Update-2004 (in Turkish). Doga Dernegi, Ankara/Turkey, p.232 (2004).
Lacaux, J.P., Y.M. Tourre, C. Vignolles, J.A. Ndione and M. Lafaye: Classification of ponds from high-spatial resolution remote sensing: Application to Rift Valley fever epidemics in Senegal. *Rem. Sen. Environ.,* **106**, 66–74 (2007).
Li, W., Z. Du, F. Ling, D. Zhou, H. Wang, Y. Gui, B. Sun and X. Zhang: A comparison of land surface water mapping using the normalized difference water index from TM, ETM+ and ALI. *J. Remote Sensing,* **5**, 5530-5549 (2013).
Lyons, E. A., Y. Sheng, L. C. Smith, J. Li, K. M. Hinkel, J. D. Lenters, J. Wang : Quantifying sources of error in multitemporal multisensor lake mapping. *Int. J. Remote Sensing,* **34**, 7887-7905 (2013).
McFeeters, S.K.: The use of the normalized difference water index (NDWI) in delineation of open water features. *Inter. J. Rem. Sen.,* **17**, 1425-1432 (1996).
Mutlu, H., S. Kadir, and A. Akbulut: Mineralogy and water chemistry of the Lake Acigol, Denizli, Turkey. Carbonates and Evaporites 14(2),191-199 (1999).
NSIDC http://nsidc.org/data/docs/daac/nsidc0184_smex_ndvi_ndwi.gd.html (2002), (11/4/2013).
Ouma, Y. and R. Tateishi: A water index for rapid mapping of shoreline changes of five east African rift valley lakes: An empirical analysis using Landsat TM and ETM+ data. *Int. J. Remote Sens.,* **27**, 3153–3181 (2006).
Ozturk, M. and O. Secmen: Ecology of wetlands. *Nature and Man,* **2**, 31-32 (1986).
Ozturk, M., O. Secmen and E. Leblebici: Plants and pollutants in the Eber lake. Ekoloji, **20**, 14-16 (1996).
Reis, S. and H.M. Yilmaz: Temporal monitoring of water level changes in Seyfe lake using remote sensing. *Hydrol. Process.,* **22**, 4448–4454 (2008).
Rogers A.S. and M.S. Kearney: Reducing signature variability in unmixing coastal marsh Thematic Mapper scenes using spectral indices. *Inter. J. Rem. Sen.,* **20**, 2317–2335 (2004).
Sener, E., A. Davraz and S. Sener: Investigation of Aksehir and Eber lakes (SW Turkey) coastline change with multitemporal satellite images. *Water Res. Manag.*, **24**, 727–745(2009).
Soti, V., A. Tran, J.S. Bailly, C. Puech, D.L. Seen and A. Begue: Assessing optical earth observation systems for mapping and monitoring temporary ponds in arid areas. *Int. J. Appl. Earth Obs. Geoinf.,* **11**, 344–351 (2009).
Sun, F., W. Sun, J. Chen and P. Gong: Comparison and improvement of methods for identifying waterbodies in remotely sensed imagery. *Int. J. Remote Sensing,* **33**, 6854-6875 (2012).
Thornthwaite, C.W.: An approach toward a rational classification of climate. *Geographical Review*, **38**, 55–94 (1948).
Thomas J. and C. Michael: SMEX02 Iowa satellite vegetation and water index (NDVI and NDWI) data. Boulder, CO: National Snow and Ice Data Center, Digital Media (2003).
Xiao, X., S. Boles, S. Frolking, W. Sala, B. Moore, C. Li, L. He and R. Zhao: Landscape-scale characterization of cropland in China using vegetation and Landsat TM images. *Inter. J Remote Sensing*, **23**, 3579-3594 (2002).
Xu, H.: Modification of normalized difference water index (NDWI) to enhance open water features in remote sensed imagery. *Inter. J. Rem. Sen.,* **27**, 3025-3033 (2006).
Varol, S. and A. Davraz: Assessment of geochemistry and hydrogeochemical processes in groundwater of the Tefenni plain (Burdur/Turkey). *Environ. Earth Sci.*, **71**, 4657-4673 (2014).
Verdin, J.P.: Remote sensing of ephemeral water bodies in Western Niger. *Int. J. Remote Sens.,* **17**, 733–748 (1996).
Yildirim, U., S. Erdogan and M. Uysal: Changes in the coastline and water level of the Aksehir and Eber lakes between 1975 and 2009. *Water Res. Manag.,* **25**, 941-962 (2011).
Zhang, W., Q. Lu, Z. Gao and J. Peng: Response of remotely sensed Normalized Difference Water Deviation Index to the 2006 drought of eastern Sichuan basin. *Sci. China Series D-Earth Sci.*, **51**, 748–758 (2008).
Zhao, X., A. Stein, X. Chen and L. Feng: Modeling spatial-temporal change of Poyang lake marshland based on an uncertainty theory random sets. *Proc. Environ. Sci.,* **3**, 105-110 (2011).